Title

A sustained intravitreal drug delivery system with remote real time monitoring capability

Authors

Hou, Huiyuan
Nieto, Alejandra
Belghith, Akram
et al.

Publication Date

2015-09-01

DOI

10.1016/j.actbio.2015.06.012

Peer reviewed

HHS Public Access

Author manuscript

Acta Biomater. Author manuscript; available in PMC 2016 September 15.

Published in final edited form as:

Acta Biomater. 2015 September 15; 24: 309–321. doi:10.1016/j.actbio.2015.06.012.

A sustained intravitreal drug delivery system with remote real time monitoring capability

Huiyuan Hou[1], **Alejandra Nieto**[2], **Akram Belghith**[1], **Kaihui Nan**[1], **Yangyang Li**[2], **William R. Freeman**[1], **Michael J. Sailor**[2], and **Lingyun Cheng**[1]

[1]Jacobs Retina Center/Shiley Eye Center at University of California, San Diego

[2]Department of Chemistry and Biochemistry, University of California, San Diego

Abstract

Many chorioretinal diseases are chronic and need sustained drug delivery systems to keep therapeutic drug level at the disease site. Many intravitreal drug delivery systems under developing do not have mechanism incorporated for a non-invasive monitoring of drug release. Current study prepared rugate porous silicon (pSi) particles by electrochemical etching with the currents frequency (K value) of 2.17 and 2.45. Two model drugs (Rapmycin and Dexamethasone) and two drug-loading strategies were tested for the feasibility to monitor drug release from the pSi particles through a color fundus camera. The pSi particles (k=2.45) with infiltration loading of rapamycin demonstrated progressively more violet color reflection which was negatively associated with the rapamycin released into the vitreous ($r=-0.4$, $p<0.001$, pairwise). In contrast, pSi with K value of 2.17 demonstrated progressive color change towards green and a weak association between rapmycin released into vitreous and green color abundance was identified ($r=-0.23$, $p=0.002$, pairwise). Dexamethasone was covalently loaded on to the fully oxidized pSi particles that appeared in vitreous as yellow color and fading over time. The yellow color decrease over time was strongly associated with the dexamethasone detected from the vitreous samples ($r=0.7$, $p<0.0001$, pairwise). These results suggest that engineered porous silicon particles may be used as a self-reporting drug delivery system for a non-invasive real time remote monitoring.

Keywords

Intravitreal drug delivery; Porous silicon; Drug release monitoring; rapamycin; dexamethasone; rabbit eye; photonic crystal

Correspondence to: Lingyun Cheng, MD, Department of Ophthalmology, Jacobs Retina Center at Shiley Eye Center, University of California, San Diego, 9415 Campus Point Drive, La Jolla, CA 92093-0946. Tel: 858-534-3780; Fax: 858-534-7985 l1cheng@ucsd.edu.

Disclosure: W.R. Freeman, Spinnaker Biosciences (C, I); M.J. Sailor, Spinnaker Biosciences (I); L. Cheng, Spinnaker Biosciences (C, I)

1. Introduction

With improved health care and advanced technology for medical discoveries, human life expectancy is steadily increasing. However, a worldwide aging population also presents us with challenges in medical care including eye disease management. For example, age-related macular degeneration has become a major health problem globally with an estimated 25 million people suffering from this disease. [1] Diabetes is also rising with aging; an estimated 285 million people have diabetes in 2010 and prevalence of diabetic retinopathy is nearly 25% if their diabetic history exceeds 15 or more years. [2] For those with chronic and refractory illness originating from the back of the eye, topical or systemic drug administration has been problematic due to either under-therapeutic drug level at the disease site or systemic side effects. Therefore, intravitreal injection of therapeutics has become a standard care procedure for these diseases. [3-6] Intravitreal injection has an advantage in comparison to systemic, topical, and periocular routes in that it places the therapeutic near the disease site—bypassing the various ocular barriers. With the availability of small gauge needles and advanced microsurgical techniques, intravitreal injection is significantly less invasive than surgical drug depot implants such as Ozurdex, Vitrasert, and Retisert. [7] [8] [9]

Although intravitreal injection is effective and well tolerated, ubiquitous short vitreous half-life of injectable therapeutics necessitates repeated injections, which introduces high risk of severe complications. [10] To extend vitreous half-life and alleviate the need for frequent injections, a variety of drug delivery systems have been proposed, including liposomes[11], nano/microspheres[12], micelles[13] as well as porous silicon particles[14-16] [17]. With extended residence time in the eye comes a need to understand the complex ocular pharmacokinetics of the drug and delivery system, which demands a large number of animals and significant investment in research effort and resources. A drug delivery system that offers non-invasive, real-time ocular drug monitoring would greatly facilitate the determination of dosing intervals. Porous silicon can be prepared in the form of multi layers (in particular, rugate filters) of varying optical density, yielding an intense reflectivity peak at a predetermined wavelength.[18-20] The wavelength of the reflectivity peak depends on the refractive index of each layer, which in turn depends on the amount of material (drug, silicon, silica, etc) contained within each of the porous layers. This property has been used to monitor the loading and release of various biomolecules [21] [22] [23, 24], and in addition to monitor the degradation of the porous silicon or porous silica host material in aqueous media [25-27]. Along with the spectral shift, the intensity of light reflected from these structures also changes as they degrade and/or release a molecular payload. The intensity of reflected light is determined by three factors: (1) the differential index (index contrast) of the layers, (2) the angle of observation relative to the angle of incident light and the surface normal, and (3) the degree of surface roughness of the particle [28, 29]. We have previously demonstrated that daunorubicin loading and release can be monitored by such reflectance measurements *in vitro* [30], and that these changes are manifested in an apparent spectral change that can be monitored by digital photography [25, 30]. The human eye is a unique organ in that it is composed of clear media that is easily probed optically and non-invasively via an external imaging system. In this work we hypothesized that we could

monitor the change in spectral properties of intravitreally administered, drug-loaded porous silicon particles, and use either the intensity or color of light reflected from the particles as a measure of intravitreal drug release using a consumer digital camera coupled to a fundus camera system. In the current study, we used porous silicon particles with two types of drug loading strategies and model drugs rapamycin and dexamethasone to test our hypothesis for this pSi sustained drug release system [31] [32] [33].

2. Materials and Methods

2.1.Synthesis of porous silicon (pSi) microparticles

Porous Si (pSi) microparticles were prepared by anodic electrochemical etch of highly doped, (100)-oriented, p-type silicon wafers (Fiber Optic Center Inc., boron-doped) in an electrolyte consisting of a 3:1 (v:v) solution of 48% aqueous hydrofluoric acid (HF) and ethanol (Fisher-Scientific, Pittsburg, PA). A Si wafer with an exposed area of 8.0 cm^2 was contacted on the backside with a strip of aluminum foil and mounted in a Teflon etching cell that was fitted with a platinum counter-electrode. The wafer was etched using a current density waveform[30]: $J = A_0 + A \cdot \cos(kt+\alpha)$, where J is applied current density, A_0 is current density offset (mA/cm^2), A is current density amplitude (mA/cm^2), k is frequency (s^{-1}), t is time (s), and α is phase shift (s^{-1}). The values used for A_0, A, and α were 90.2 mA/cm^2, 12.4 mA/cm^2, and 0, respectively. The current density waveform generates a porosity modulation in the porous silicon layer that acts as a 1-dimensional photonic crystal. The photonic crystal displays a sharp peak (stop band of the photonic crystal) in the optical reflectance spectrum whose wavelength is directly proportional to k. In order to obtain particles that displayed colors having good contrast against the rabbit fundus, k values were systematically changed in order to generate reflectance peaksin the blue to green region of the spectrum (450-560 nm). The waveform was etched into the silicon wafer for a total of 400 s. The resulting porous layer was then removed from the silicon substrate by replacing the electrolyte with a 1:29 (v:v) solution of 48% aqueous HF and ethanol and then applying an anodic pulse (6.2 mA/cm^2) for 120 s. This latter step, referred to as “electropolishing” or “liftoff” in the literature, undercuts the porous layer and detaches it from the silicon substrate. The etching and electropolishing procedure was repeated 20 times per wafer. The particles were harvested every 4 etches and the resulting porous layers were dispersed in ethanol and placed in small vials, which were subjected to ultrasonication (Model FS5 dual action ultrasonic cleaner, Thermo Fisher Scientific, Pittsburg, PA) for 30 min to form the microparticles. After ultrasonic treatment, the supernatant was removed and the particles were resuspended in fresh ethanol. The particles were washed with ethanol three times until the supernatant was transparent.

2.2. Reflectance measurements to select the optimal particle color

The particle synthesis was optimized to obtain colors in the yellow or green region of the spectrum, so they would display maximal contrast against the red color of the retina in the digital images. Because the wavelength of the stop band is sensitive to the refractive index of the material filling the pores, the optical reflection spectrum was measured in various media (air, deionized water, and aqueous PBS buffer solution) [34] and the k value from above was systematically varied to obtain stop band wavelengths that could be predicted to

fall in the yellow-green region of the spectrum when the particles were immersed in vitreous fluid. The k values 2.45 and 2.17 were selected for the current studies, which, after oxidation and immersion in rabbit vitreous, appeared violet and green, respectively. The particle thickness and open porosity were also calculated by optical measurements of the reflectivity spectrum on the porous layer as a function of liquid infiltration (SLIM, or Spectroscopic Liquid Infiltration Method) [34, 35].

2.3.1. Rapamycin loading by infiltration and loading efficiency—Microparticles with *k* values of 2.45 and 2.17 were used for rapamycin (Rap) infiltration loading. The resulting drug-loaded particles are denoted as particle 2.45-inf-RAP and 2.17-inf-RAP, respectively. The $pSiO_2$-C8 formulation was prepared from pSi by air oxidation followed by silanization with an organosilane containing a pendant C8 hydrocarbon, methoxy(dimethyl)octylsilane: The samples were placed in a ceramic boat inside a muffle furnace (Thermo Fisher Scientific, Pittsburg, PA), ramped from room temperature to 600 °C at a rate of 10 °C/min, held at 600 °C for 1 hour and cooled back to room temperature. In order to generate Si-OH terminated surfaces for further coupling of the organosilane, the partially oxidized pSi particles were treated with 4% (v/v) aqueous hydrochloric acid (diluted from 37 wt% aqueous HCl; Sigma-Aldrich), shaken for 1 hour at room temperature and washed with deionized water. Approximately 40 mg hydroxyl-terminated $pSiO_2$ microparticles were suspended in ethanol, transferred to a Schlenk flask and dried under vacuum overnight. Then 8.3 mmol of methoxy(dimethyl)octylsilane (98 wt%; Sigma-Aldrich) per gram of pSi microparticles were dissolved in anhydrous toluene and added with a syringe under nitrogen flow to yield an 8 wt% final solution. The flask was heated at 120 °C in a nitrogen atmosphere and allowed to react overnight with constant shaking. The particles were then washed with toluene (Sigma-Aldrich), dimethylformamide (Sigma-Aldrich), ethanol (Fisher-Scientific) and ether (Sigma-Aldrich), three times each and stored in a desiccator. This procedure results in porous silica with eight-carbon atom alkyl chains covalently grafted to the surface ($pSiO_2$-C8) [36, 37]. Surface chemistry was characterized by attenuated total reflectance Fourier transform infrared (ATR-FTIR) spectroscopy on a Nicolet 6700 spectrometer fitted with a Smart-iTR ATR attachment (Thermo Fisher Scientific, Pittsburg, PA). Approximately 20 mg functionalized pSi microparticles were transferred to a glass vial sealed with a rubber septum and placed under vacuum (< 0.002 atm) for approximately 30 minutes. Thereafter, connection to the vacuum pump was closed and 0.4 mL of an infiltrating solution of 50 g/L rapamycin (RAP; LC Labs, Woburn, MA) in acetone (HPLC grade; Sigma-Aldrich, St Louis, MO) was injected into the vial. The infiltrating liquid flowed rapidly into the pores of pSi microparticles, which were left to soak in the liquid for 10 minutes before breaking the vacuum. The vials were tightly closed with a cap, protected from direct sunlight with aluminum foil wrapping and placed in a rotator shaker at 20 rpm (position 40, Model 24; Reliable Scientific, Inc. Nesbit, MS) at room temperature overnight. The supernatant was aspirated with a pipette and the particles were dried at room temperature and stored under vacuum avoiding further oxidization.

The mass loading efficiency of drug into the $pSiO_2$–C8 microparticles was determined by positive ion mode electrospray ionization (ESI) liquid chromatography-mass spectrometry

(LC-MS/MS) in an Agilent 1260 HPLC chromatographic system coupled with a Thermo LCQdeca-MS spectrometer [32].

2.3.2. Dexamethasone loading by covalent attachment and loading efficiency

—Microparticles with *k* value of 2.17 were used for dexamethasone (Dex) loading, denoted as particle 2.17-cov-DEX. Dex was loaded into pSi microparticles through covalent attachment by creating a chemical bond between the drug and functional groups on the particle surface [38]. Briefly, pSi particles were thermally oxidized at 800 °C before treatment with a 2% aqueous HCl solution. The particles were then vortexed in a solution 1% in 3-aminopropyltrimethoxysilane (Sigma-Aldrich) before the amine-functionalized porous SiO_2 particles were reacted with 0.1 M succinic anhydride (99%, Sigma-Aldrich) in N,N-dimethylformamide (DMF, Sigma-Aldrich) to obtain a carboxylic acid functional surface ($pSiO_2$-CO_2H). After activation of the surface carboxyl species with dicyclohexylcarbodiimide (DCC) in dichloromethane (DCM), 4 mg of free Dex (Sigma-Aldrich) was added and the tube was sealed with parafilm, protected from direct sunlight with aluminum foil wrapping and rotated at room temperature for 7 days. After the loading procedure, the particles were pelletized by centrifugation and rinsed with DCM and ethanol five times to remove unloaded drug and any excess linkers. The presence of the functional linker on the particle surface and the successful covalent attachment of Dex to the microparticles was confirmed by ATR-FTIR [38].

Dex loading efficiency was analyzed by thermogravimetry (TGA) as shown previously [16]. The $pSiO_2$-CO_2H ($pSiO_2$ with carboxylic acid functional surface) and 2.17-cov-DEX ($pSiO_2$ containing Dex covalently attached to the pore walls) samples (2 mg each) were placed in two 90 μL alumina sample cups respectively. Samples were heated at a constant rate of 10°C/minute up to 800 °C in nitrogen atmosphere with a purge rate of 10 mL/min using a Q600 simultaneous TGA/DSC apparatus (TA Instruments, New Castle, DE). Weight percent loading efficiency of Dex in the samples was determined by comparison of the TGA curves from $pSiO_2$-CO_2H and $pSiO_2$-COO-Dex.

2.4. In vitro drug release and color monitoring

The 2.45-inf-RAP microparticle formulation was selected for a pilot *in vitro* study to monitor the correlation of color change with drug release. Particles (2mg) were suspended in 4.5mL (the approximate volume of vitreous in the human eye) Hank's buffered saline solution (HBSS, without calcium and magnesium) and added to a 35×10mm plastic petri dish, which was sealed with paraffin film, protected from light with aluminum foil wrapping, and maintained at 37 °C. Six identical petri dishes were set up, three for observation of surface structure and three for color monitoring. Using an optical microscope (Olympus SZH, Olympus, Japan) with a coaxial halogen cold light illumination source (brightness-6/3350K, filter-daylight, Leica KL 2500 LCD, Otto-Schott-Str, Germany) and a digital camera (Canon EOS Rebel T2i, Canon, Japan), particle images were recorded at time points of 3, 6, 9, 24, 48, 72, 96, 120, and 168 hours. A majority of the particles in each petri dish were captured, and the same camera settings (F-stop: f/16, exposure time: 1/20 sec, ISO: 400, no flash), magnification (600x) and indoor lighting conditions were used throughout the study. Immediately after image acquisition at each time point and for each

dish, 1mL of the supernatant was sampled by syringe (30-gauge needle) and stored at -80 °C until quantification. After each sample, an equal amount of fresh HBSS was carefully added to the dish to replace the volume removed. Rap released from the particles into the sampled supernatant was quantified using HPLC-MS/MS. The supernatants were centrifuged at 13,000rpm for 10 min to remove any particles inadvertently introduced during sampling, and 100 uL of the supernatant was subjected to HPLC-MS/MS analysis (Agilent 1260 HPLC chromatographic system coupled with a Thermo LCQdeca-MS spectrometer) as described previously [37]. Under the analytical conditions, rapamycin showed a retention time of 13.1 minutes and the internal standard, ascomycin, showed a retention time of 12.4 minutes.

2.5. Evolution of particle surface structure during drug release

Changes in surface structure, in particular surface roughness on the micron scale, has an effect on the angular dependence of the reflectance spectrum. To monitor these changes as a function of the particle degradation process, the 2.45-inf-RAP particles were sampled from three petri dishes on day 3 and again on day 21. Particles were rinsed twice with deionized water and 3 times with ethanol before being dried completely in vacuum. The surface of the particles was observed by scanning electron microscope (SEM) using a Phillips XL30 field emission electron microscope operating at an accelerating voltage of 5 kV (FEI Phillips, Hillsboro, OR). At least 3 images were captured from each sample from each petri dish at each time point. The resulting images were analyzed by Image J (National Institutes of Health) to quantify the degree of surface roughness by detecting arithmetical mean deviation (Ra), skewness (Rsk), and kurtosis of the roughness profile (Rku).

2.6.In vivo drug release and color monitoring

Fifteen, fifteen, and eighteen New Zealand Red rabbits were used for *in vivo* investigation of 2.45-inf-RAP, 2.17-inf-RAP, and 2.17-cov-DEX particles, respectively. All of the animals were handled in accordance with the ARVO statement for the Use of Animals in Ophthalmic and Vision Research, and the studies were approved by the Institutional Animal Care and Use Committee (IACUC) of the University of California, San Diego. Only one eye of each animal was used for intravitreal injection. Slit lamp and indirect ophthalmoscopy were performed on all animal eyes before injection and baseline fundus images were recorded. For the intravitreal injection procedure, the rabbits were anesthetized with subcutaneous injections of 20 mg/kg ketamine and 5 mg/kg xylazine. After eye preparations for disinfection, 2 mg of each type of particle in 150μL sterile balanced salt solution (BSS) was injected into the midvitreous cavity of the right eyes under direct view of a surgical microscope following a paracentesis. Intravitreal injection was performed with a 1mL slip tip syringe and 27-gauge needle through the pars plana at a location 2 mm from the limbus. After the injection, the vial, syringe and needle were saved for mass balance purposes. The particles remaining in the vial and syringe for each rabbits were carefully recovered, rinsed with deionized water, dried in vacuum, and weighed to calculate the real injection dose. Following the injections, the eyes were examined and three rabbits each were sacrificed at day 1, 7, 14, 21 and 35 for 2.45-inf-RAP and 2.17-inf-RAP groups, and at day 3, 7, 14, 21, 28, and 35 after injection for 2.17-cov-DEX group. At each time point slit-lamp examination of the anterior segment, intraocular pressure (IOP) measurement with a handheld tonometer

(Tonopen; Medtronic, Jacksonville, FL) and fundus examinations were performed. Color fundus photographs were taken using the same camera (Canon EOS Rebel T2i, Canon, Japan) used in the *in vitro* study at each exam with camera settings of F-stop: f/16, exposure time: 1/20 sec, ISO: auto, no flash. Indoor light sources were consistent through the entire study period. Multiple fundus images were acquired from each exam for image analysis. Three rabbits at each time point were sacrificed for vitreous drug quantitation following image acquisition. Whole vitreous was dissected as previously described [16] and centrifuged for 20 min at 5,000 rpm/min, while the vitreous supernatant was subjected to HPLC/MS/MS in an Agilent 1260 HPLC chromatographic system coupled with a Thermo LCQdeca-MS spectormeter for drug quantitation. Acetonitrile (Sigma-Aldrich, HPLC-grade) was used to pre-treat the vitreous supernatant before HPLC analysis [39]. Rap or Dex in 100 μL vitreous supernatant was quantitated by spiking 1ng of ascomycin or 100ng of katorolac into the samples. After extraction, the extracts were dried in a speed-vac concentrator (Savant SpeedVac DNA110, Thermo-Savant, Holbrook, NY) and re-suspended in 100 μL of mobile phase prior to injection (10~20 μL) into the chromatographic column. A LC-ESI-MS/MS run of normal vitreous supernatant was used as a blank control.

2.7. Image extraction and statistical analysis

Colors from in vitro and in vivo images were extracted into an RGB color model, which was then quantitated in area and intensity using a custom written code in the MATLAB program (MATLAB R2013a, Mathworks, Natick, MA). We used Bayesian theory to estimate the location of the particles and their colors. Specifically, for each RGB channel, the particles were statistically modeled as zero-mean Bernoulli-Gaussian sequence; i.e, the particle locations are independently distributed with probability $\lambda>0$ (Bernoulli sequence), and their color components in the RGB model were Gaussian distributed with mean zero and standard deviation $\sigma>0$. Using the RGB model, the real color of each particle(i) can be represented with the triplet (R(i) , G(i), B(i)) where (R(i) , G(i) B(i)) $\in$ ([0,255])3. For example the triplet of a pure green particle is equal to (0,255,0). In this study, we defined 4 color classes. Each class is defined by its centroid C: 1) the green class Cg=(80,80,30), 2) the yellow class Cy=(190,190,50), 3) the violet class Cv=(100,50,50), and 4) the blue class Cb=(10,10,200). The centroids were selected empirically in a way that they can cover most of the spectrum of each class. The real color of each particle was then assigned to one of the four color classes based on the distance of its triplet (R(i) , G(i), B(i)) to the centroids. Finally, for each image we quantified the number of pixels belonging to each class. Because the observed colors of the particles depend on their position given the camera (e.g, a particle oriented at an angle such that it does not give a specular reflection to the camera will have black color), we acquired at least 10 images at each follow-up exam. Moreover, for *in vitro* and *in vivo* drug release the data were normalized actual injected drug from the mass balance calculation. The association between the color changes and the drug levels in vitreous was analyzed using pariwise correlation. To assess *in vivo* safety, ophthalmic data such as IOP readings were recorded multiple times at different time points from both eyes of the same animal using the paired t test. All analyses were performed using JMP statistical software (version 10; SAS Institute Inc. Cary, NC) and p-values smaller than 0.05 were considered to be significant.

3. Results

3.1. Selection of optimal spectral properties of pSi particles

The sharp reflectivity peak generated by the rugate optical filter structure gives the particles a distinctive color. The particle sizes were shown in table 1. We first optimized this color such that it would show up in strong contrast against the red background of the fundus. We prepared a range of particles with reflectance peaks spanning a range of wavelengths and quantified the reflectance spectra in various media using SLIM (spectroscopic liquid infiltration method). For experimental convenience, the measurements were performed on porous layers that had not been removed from the silicon substrate, such that they were flat and easy to orient relative to the spectral axis. Each measurement was repeated at least seven times. The average wavelength of the reflectivity peaks and their corresponding apparent visible colors for each type of fresh or oxidized pSi film in different media and their corresponding reflective shifts are summarized in Table 2. The particles with *k* value of 2.17 and 2.45 were chosen for the current study because they were estimated to display green or violet (respectively) in rabbit vitreous.

3.2.Selected particle parameters and drug loading efficiency

Three optimized porous Si particle formulations were chosen for detailed *in vitro* and *in vivo* study. Their key parameters are summarized in Table 2. Of the two drugs used in the study, Dex was grafted to the inner pore walls of its pSi formulation by covalent bonding using standard aminosilanol linker chemistries (termed “covalent” loaded), whereas Rap was loaded into its two pSi formulations by simple physisorption to the inner pore walls of material that had been previously surface-modified with hydrophobic C8 hydrocarbon chains (termed “infiltration” loaded).

The presence of the functional linker on the particle surface and the successful covalent attachment of Dex to the microparticles were confirmed by ATR-FTIR [31]. The mass loading efficiency of Rap was determined by HPLC-MS/MS; Dex loading efficiency was calculated by TGA. As shown in Table 3, mass loading efficiency for both methods was in the range 6-10%.

3.3.In vitro color shifting of pSi versus drug release

To evaluate the self-reporting aspects of the drug delivery system in this study, we immersed the 2.45-inf-RAP particle type in HBSS at 37 °C in a petri dish and quantified the color change and the amount of drug released into the medium as a function of time (Figure 1 and Figure 2). The images recorded by the camera showed a gradual increase in the green color component while the violet component gradually decreases. The drug leaches out of this formulation more rapidly than the measured color changes. These color changes are not overtly perceptible by simple visual inspection of the images (Figure 1). The similar setting and testing was conducted for covalent drug loading strategy using 2.17-cov-DEX particles (Figure 2).

3.4. Surface roughness of pSi microparticles during drug release in aqueous medium

Surface structural (roughness) changes in the pSi particles during the aqueous *in vitro* drug release study was examined by SEM and quantified by images analysis (Figure 3), in order to understand the relationship between roughness profile and the observed spectral properties of the particles. The surface of the particles displayed a consistent increase in surface roughness, corresponding to a noticeable enlargement of surface pits. Before immersion in the aqueous media, the surface was relatively smooth, with few features larger than 500 nm. Larger pits and pores in the surface were evident after 3 days in media, and by day 21 many micron-scale surface features were evident. A model system was fabricated to investigate the effect of surface roughness on the intensity and wavelength of the reflectance spectrum. A photonic crystal was prepared and then spray-coated with polystyrene microdroplets following the published procedure [40] to form an artificially roughened surface. In contrast to the corrosion-induced roughening that occurs upon aqueous degradation, the polymer droplets on the surface induce only a minor change in the wavelength of the stop band, allowing more direct comparison of the spectral dependence of reflected angle on surface roughness. The smooth surface showed a strong specular reflectance that decayed very rapidly as the detector moved off of the specular axis, becoming undetectable at angles >1 degree from the specular axis (Figure 4). By contrast, the artificially roughened surface scattered intensity over a substantially larger solid angle, detectable at angles up to 9 degrees from the specular axis. The wavelength of the stop band also varied as a function of angle. The roughened surface displayed a less pronounced shift in wavelength with angle, compared to the smooth surface.

3.5. In vivo spectral and drug release properties of pSi microparticles

3.5.1. Evolution of color of 2.45-inf-RAP particles *in vivo*—One day after intravitreal injection, the 2.45-inf-RAP pSi particles appear as a dark mass with a predominantly violet color against the retinal background (Figure 5). As time progressed, the proportion of dark particles decreased (Figure 5), and a larger quantity of particles appeared with a violet color over a period of 5 weeks (Figure 5). The vitreous RAP levels at day 1 were highest, at 27 ng/mL, decaying to near zero by day 23 (Figure 6), and this drug concentration was correlated with the increase in the violet color channel ($r=-0.4$, $p<0.001$, pairwise).

3.5.2. Evolution of color of 2.17-inf-RAP particles *in vivo*—The 2.17-inf-RAP particles differed from the 2.45-inf-RAP particles in that the k = 2.17 formulation was selected to display a green color (rather than violet) in the rabbit vitreous. Similar to the 2.45-inf-RAP particles, one day after intravitreal injection, the 2.17-inf-RAP pSi particles appear as a dark mass with a predominantly green color against the retinal background (Figure 7). As with the violet color of the 2.45-inf-RAP particle formulation, as time progressed, the proportion of dark particles decreased (Figure 7), and a larger quantity of particles appeared with the characteristic green color of this formulation over the 5-week period of observation (Figure 7). The vitreous RAP levels at day 1 were highest, at 40 ng/mL, decaying to near zero by day 23 (Figure 8), and this drug concentration was weakly correlated with the increase in the green color channel ($r=-0.23$, $p=0.002$, pairwise).

3.5.3. Evolution of color of 2.17-cov-DEX particles *in vivo*—In contrast to the particles loaded by simple infiltration of rapamycin into the carrier particle (2.45-inf-RAP and 2.17-inf-RAP), the drug in the 2.17-cov-DEX formulation was loaded by covalent grafting of the drug to the inner pore walls of the carrier particle. In addition, the carrier particle for the infiltration-loaded formulations was distinctly more hydrophobic, as it contained a C8 hydrocarbon surface instead of the carboxylic acid/amide surface that link dexamethasone to the surface in the covalent formulation. The overall appearance of the 2.17-cov-DEX formulation was yellow after injection into the rabbit eye, which faded in intensity (Figure 9) and shifted in color somewhat to the blue (Figure 10) as the pSi particles degraded and released the payload during the 5-week observation period. The yellow color decrease over time was strongly associated with the dexamethasone detected from the vitreous samples ($r=0.7$, $p<0.0001$, pairwise). Compared with the 2.45-inf-RAP and 2.17-inf-RAP formulations, the number of 2.17-cov-DEX formulation particles present in the rabbit eye noticeably decreased during the 5-week study.

During clinical follow-up examinations, no abnormality was noted in either anterior or posterior segments of the eye.

Discussion

Intravitreal administration of various therapeutics has now become a standard procedure with the advent of anti-VEGF agents and numerous large-scale clinical trials. However, the necessity of frequent intravitreal injections has become an emotional and financial burden for both patients and physicians. This has led to an intense search for injectable or implantable delivery systems that are tolerated by the eye, to extend the therapeutic window. In addition, due to patient-to-patient variability of administered dose and metabolic processing of therapeutic systems, it is desired that the delivery system possess an ability to non-invasively report on the quantity of drug released or the residual drug capacity. Among the several delivery systems (polymer nanoparticles, micro particles, micelles and liposomes) under investigation and development, [41] [42] [43] porous Si has the advantage in that it can be degraded into soluble silicic acid in vitreous and cleared along with intraocular fluid turnover[44]. In addition, its photonic spectrum can be correlated with residual drug in the nanostructure [30]. Although this self-reporting property has been demonstrated *in vitro*, prior to this study it had not been demonstrated in the living eye. However it should be noted that the *in vivo* sensing aspects of porous Si have been demonstrated in live animal eyes in the form of ocular pressure actuators [45]. The current study was designed to test the feasibility of the self-reporting drug delivery aspect of the porous Si system.

The color of the particles derives from a one-dimensional photonic crystal that is embedded in the particles in the form of a periodic porosity gradient [46]. The repeating high to low porosity pattern in the particle acts as a dielectric stack, the spacing of which is set by the periodicity of the electrochemical current used in the preparation of the material—higher currents yield higher porosity and lower currents yield lower porosity. The color is also determined by the refractive index of each layer. Because the particles are porous, the refractive index of the layers varies depending on the material filling the pores and the

refractive index of the host nanostructure. The color is also dependent (to a lesser degree) on observation angle (Figure 4). An initial set of optimizations on the particle manufacture were performed to yield particles whose colors would show up in stark contrast to the retinal background, to make quantification with a commercial color camera easier. For a clinical application, the color of the particles might have to be tuned to the near infrared region of the spectrum and observed with a NIR camera to avoid perception by the patient.

Once in the vitreous, the predominant reason for a color change is the oxidation of residual silicon (index 3.1) in the skeleton to silicon dioxide (index 1.5-1.7) and the subsequent dissolution of the silicon dioxide skeleton [30]. At the 10% loading of drug used in this work, the leaching of drug may not change the color of the particles appreciably (< 10nm spectral shift) because any drug removed is replaced with vitreous fluid, which has a similar refractive index [30]. For the 2.45-inf-RAP and 2.17-inf-RAP formulations, the C8 surface chemistry used in the preparation imparts a significant hydrophobic nature to the particles, which increases their stability in aqueous media. In these images, the degradation is manifested as a distinctive enlargement of the pores and pitting of the surface. This pitting may generate a large change in the intensity of the characteristic color of the particles due to enhanced scattering.

The reason for the increased intensity of the characteristic color reflected from the photonic crystal derives from the fact that they are one-dimensional photonic crystals—that is, they only reflect the characteristic color of the particle along a direction normal to the layers (perpendicular to the face of the particles). As shown in Figure 4, the intensity of light reflected from a smooth (as-formed) porous Si layer is highly directional, and it falls off very rapidly once the angle of observation deviates from the specular reflection angle. In the model system of Figure 4, the reflected color becomes undetectable to the CCD spectrometer for angles > 0.5 degrees off specular. Roughening of the surface (at the micron scale) distributes the intensity of scattered light over a much greater solid angle (> 9 degrees in the test system) [40]. Similarly, the corrosion of the pSi matrix generates surface scattering centers that increase the range of angles at which the particles are observable. The overall result is that corrosion of the particles effectively makes them more visible to the fundus camera. For example, the fundus images obtained only 1 day after injection of particles (Figures 5 and 7) display many “dark” particles, which are just particles that are oriented such that their specular reflection is not within the acceptance cone of the camera lens or stacked and so the strong absorbance of the black silicon matrix is all that is perceived by the camera. The few particles that are less than 1 degree off of the specular reflection axis are perceived as green. In subsequent weeks, the particles gradually disperse and the portion of the particles that appear dark decreases, while the violet or green color characteristic of the photonic crystal increases in prevalence (Figures 5 and 7, respectively). This increase in the portion of violet or green particles is attributed to the roughening of the pSi particle surface and consequent increase in the angles over which the particles scatter their characteristic color. Incidentally, this same spectral phenomenon has been described previously in beetle shells, which also generate an angularly dispersed color via a one-dimensional photonic crystal [47]. In the case of the beetle shell, the light scattering domains responsible for the angular dispersion are in the form of a roughened chitin layer on the outer surface of the beetle cuticle.

Because surface corrosion is responsible for the perceived increase in intensity of color from the particles, the observed changes are a poor predictor of drug release for the 2.45-inf-RAP and 2.17-inf-RAP particle formulations—where drug is loaded via simple adsorption to the inner pore walls of the particles. In these formulations drug release is not well correlated to the perceived color of the particles, and the particles themselves degrade quite slowly. By contrast, the 2.17-cov-DEX formulation shows a relatively direct correlation between the decrease in the yellow channel and the release of drug. This formulation is prepared from a fully oxidized porous Si film. The lower index of refraction of silicon oxide (1.7) relative to silicon (3.1) results in less intense structural color and less efficient scattering from surface roughness variations. Thus this particle type does not display as intense a color in the fundus images, and the transparent nature of the particles makes those particles that are not aligned with the specular axis of the camera less visible (Figure 9). Because the drug is chemically bonded to the inner pore walls of the high surface area particles, the 2.17-cov-DEX formulation can only release drug as the particle degrades. The surface chemistry of this formulation is also less stable in aqueous media, and so the particles degrade more quickly than the 2.45-inf-RAP and 2.17-inf-RAP particle formulations, leading to a much higher concentration of drug in the eye (Figures 10). At the last time point (5 weeks), 2.17-cov-DEX particles had substantial erosion and material loss that may explain the inconsistence of the correlation between drug release and color change of the particles. The infiltration-loaded formulations probably release drug via a combination of particle degradation and simple leaching into the vitreous, although both of these processes are slow due to the hydrophobic interior of the pSi matrix. To mimic a physiological condition, PBS was used as a release medium and release was kept under 37°C. The release medium was 4.5 mL and sampling volume at each time point was 1 mL. Such setting may have contributed to plateau of the release in late phase because rapmycin degrade in PBS at 37 degree. [48]

Compared to the *in vitro* experiments, the porous Si particles in the vitreous are randomly positioned in relation to the illuminating light. In an attempt to capture and quantify the color change at each time point, we took multiple images within 20 degrees of the visual axis. At least 10 frames for each eye at each time point were analyzed. To this end, we used a fully Bayesian approach to estimate the location of the particles and their colors since this approach is relatively simple and offers efficient tools to include *a priori* knowledge (e.g. the size and the location of the particles, the texture of the background) through the *a posteriori* probability density function. In particular, we used a convolution model to overcome the problem of overlapping particles. This is particularly important in order to measure small changes over time that can be hidden because of the varied locations and orientations of the different particles. An experienced physician researcher manually validated the program to ensure the correct sampling. If we identified images where the algorithm failed, a semi-supervised version of this approach was used where the doctor manually selected the particles. There are many notable limitations of the method used in this study. One of the limitations is that the researcher needs to verify the sampling to identify the occasional algorithm failures, which can be time consuming for a large database. Another limitation is that the spectral color of the particles can vary with angle (Figure 4). To overcome this problem it was important to obtain many images of the same eyes with different camera viewing angles. Additionally, a commercial camera with a simple RGB

sensor, rather than a more accurate spectrally resolved imaging spectrometer, was used to capture the images. Finally, when two or more particles are spatially superposed on each other, the observed color is the sum of each particle's reflected color, which may bias the results.

In summary, this proof of concept study demonstrated the feasibility of using changes in the observed color from porous Si photonic crystals as a surrogate measure of drug release *in vivo*. It also demonstrated the challenges associated with the method. Whereas the best correlation was observed for clear particles composed of SiO_2 in which the drug was chemically grafted to the inner pore walls, the color changes from particles containing significant silicon content and in which the drug was loaded by simple adsorption may give little predictable correlation. Though the exact contribution from drug leaching, particle degradation and other factors cannot be quantitated in this study, fundus digital images showed clear color changes which are in association with drug levels in the vitreous. This is the first such study in living eyes and can be viewed as the first steps towards the possible development of a system that may ultimately fulfil remote monitoring of drug release. The current study used visible light to demonstrate the concept; however, by changing K value the reporting light can be tuned to be out of the visible spectrum.

Acknowledgements

Financial support: This study was supported by NIH EY020617 and partially by a NIH P30 core grant P30EY022589 (Histology Module).

REFERENCES

[1]. Klein R, Klein BE. The prevalence of age-related eye diseases and visual impairment in aging: current estimates. Investigative ophthalmology & visual science. 2013; 54:ORSF5–ORSF13. [PubMed: 24335069]

[2]. Nentwich MM, Ulbig MW. Diabetic retinopathy - ocular complications of diabetes mellitus. World journal of diabetes. 2015; 6:489–99. [PubMed: 25897358]

[3]. Gillies MC, Sutter FKP, Simpson JM, Larsson J, Ali H, Zhu M. Intravitreal Triamcinolone for Refractory Diabetic Macular Edema: Two-Year Results of a Double-Masked, Placebo-Controlled, Randomized Clinical Trial. Ophthalmology. 2006; 113:1533–8. [PubMed: 16828501]

[4]. Comparison of Age-related Macular Degeneration Treatments Trials Research G. Martin DF, Maguire MG, Fine SL, Ying GS, Jaffe GJ, et al. Ranibizumab and bevacizumab for treatment of neovascular age-related macular degeneration: two-year results. Ophthalmology. 2012; 119:1388–98. [PubMed: 22555112]

[5]. Group CR, Martin DF, Maguire MG, Ying GS, Grunwald JE, Fine SL, et al. Ranibizumab and bevacizumab for neovascular age-related macular degeneration. The New England journal of medicine. 2011; 364:1897–908. [PubMed: 21526923]

[6]. Schmidt-Erfurth U, Kaiser PK, Korobelnik JF, Brown DM, Chong V, Nguyen QD, et al. Intravitreal aflibercept injection for neovascular age-related macular degeneration: ninety-six-week results of the VIEW studies. Ophthalmology. 2014; 121:193–201. [PubMed: 24084500]

[7]. Semeraro F, Russo A, Danzi P, Costagliola C. Central retinal vein occlusion treated with Ozurdex: a case report and review of literature. J Ocul Pharmacol Ther. 2013; 29:84–7. [PubMed: 22853700]

[8]. Bourges JL, Bloquel C, Thomas A, Froussart F, Bochot A, Azan F, et al. Intraocular implants for extended drug delivery: therapeutic applications. Adv Drug Deliv Rev. 2006; 58:1182–202. [PubMed: 17107737]

[9]. TABAN M, LOWDER CY, KAISER PK. Outcome of Fluocinolone Acetonide Implant (Retisert™) Reimplantation for Chronic Noninfectious Posterior Uveitis. RETINA. 2008; 28:1280–8. 10.097/IAE.0b013e31817d8bf2. [PubMed: 18628725]

[10]. Day S, Acquah K, Mruthyunjaya P, Grossman DS, Lee PP, Sloan FA. Ocular complications after anti-vascular endothelial growth factor therapy in Medicare patients with age-related macular degeneration. American journal of ophthalmology. 2011; 152:266–72. [PubMed: 21664593]

[11]. del Pozo-Rodriguez A, Delgado D, Gascon AR, Solinis MA. Lipid nanoparticles as drug/gene delivery systems to the retina. J Ocul Pharmacol Ther. 2013; 29:173–88. [PubMed: 23286300]

[12]. Christoforidis JB, Chang S, Jiang A, Wang J, Cebulla CM. Intravitreal devices for the treatment of vitreous inflammation. Mediators Inflamm. 2012; 2012:126463. [PubMed: 22988344]

[13]. Liu S, Jones L, Gu FX. Nanomaterials for ocular drug delivery. Macromol Biosci. 2012; 12:608–20. [PubMed: 22508445]

[14]. Chhablani J, Nieto A, Hou HY, Wu EC, Freeman WR, Sailor MJ, et al. Oxidized Porous Silicon Particles Covalently Grafted with Daunorubicin as a Sustained Intraocular Drug Delivery System. Investigative ophthalmology & visual science. 2013; 54:1268–79. [PubMed: 23322571]

[15]. Hartmann KI, Nieto A, Wu EC, Freeman WR, Kim JS, Chhablani J, et al. Hydrosilylated Porous Silicon Particles Function as an Intravitreal Drug Delivery System for Daunorubicin. J Ocul Pharmacol Th. 2013; 29:493–500.

[16]. Hou H, Nieto A, Ma F, Freeman WR, Sailor MJ, Cheng L. Tunable sustained intravitreal drug delivery system for daunorubicin using oxidized porous silicon. J Control Release. 2014; 178C: 46–54. [PubMed: 24424270]

[17]. Micinnes SJP, Irani Y, Lad HR, Williams KA, Voelcker NH. Porous silicon films and microparticles as a vehicle for the loading and extended release of infliximab to the eye. Eur Cell Mater. 2013; 26

[18]. Lorenzo E, Oton CJ, Capuj NE, Ghulinyan M, Navarro-Urrios D, Gaburro Z, et al. Porous silicon-based rugate filters. Appl Optics. 2005; 44:5415–21.

[19]. Thonissen M, Berger MG, Theiss W, Hilbrich S, Kruger M, Luth H. The colourful world of porous silicon: From interference filters to applications. Solid State Phenom. 1997; 54:65–72.

[20]. Berger MG, Arens-Fischer R, Thoenissen M, Krueger M, Billat S, Lueth H, et al. Dielectric filters made of porous silicon: advanced performance by oxidation and new layer structures. Thin Sol Films. 1997; 297:237–40.

[21]. Chan S, Horner SR, Fauchet PM, Miller BL. Identification of gram negative bacteria using nanoscale silicon microcavities. J Am Chem Soc. 2001; 123:11797–8. [PubMed: 11716737]

[22]. Dancil KPS, Greiner DP, Sailor MJ. A porous silicon optical biosensor: Detection of reversible binding of IgG to a protein A-modified surface. J Am Chem Soc. 1999; 121:7925–30.

[23]. Li YY, Cunin F, Link JR, Gao T, Betts RE, Reiver SH, et al. Polymer replicas of photonic porous silicon for sensing and drug delivery applications. Science. 2003; 299:2045–7. [PubMed: 12663921]

[24]. Dhanekar S, Jain S. Porous silicon biosensor: current status. Biosens Bioelectron. 2013; 41:54–64. [PubMed: 23122704]

[25]. Ariza-Avidad M, Nieto A, Salinas-Castillo A, Capitan-Vallvey LF, Miskelly GM, Sailor MJ. Monitoring of degradation of porous silicon photonic crystals using digital photography. Nano Res Lett. 2014; 9:410.

[26]. Wu EC, Andrew JS, Cheng L, Freeman WR, Pearson L, Sailor MJ. Real-time Monitoring of Sustained Drug Release using the Optical Properties of Porous Silicon Photonic Crystal Particles. Biomaterials. 2011; 32:1957–66. [PubMed: 21122914]

[27]. Cheng L, Anglin E, Cunin F, Kim D, Sailor MJ, Falkenstein I, et al. Intravitreal properties of porous silicon photonic crystals: a potential self-reporting intraocular drug delivery vehicle. Br J Ophthalmol. 2008; 92:705–11. [PubMed: 18441177]

[28]. Sailor, MJ.; Schwartz, MP.; Alvarez, S.; Bhatia, S.; Derfus, A.; Migliori, B., et al. Porous photonic crystal with light scattering domains and methods of synthesis and use thereof. issued2011

[29]. Schwartz MP, Derfus AM, Alvarez SD, Bhatia SN, Sailor MJ. The smart petri dish: A nanostructured photonic crystal for real-time monitoring of living cells. Langmuir. 2006; 22:7084–90. [PubMed: 16863264]

[30]. Wu EC, Andrew JS, Cheng L, Freeman WR, Pearson L, Sailor MJ. Real-time monitoring of sustained drug release using the optical properties of porous silicon photonic crystal particles. Biomaterials. 2011; 32:1957–66. [PubMed: 21122914]

[31]. Wang C, Hou H, Nan K, Sailor MJ, Freeman WR, Cheng L. Intravitreal controlled release of dexamethasone from engineered microparticles of porous silicon dioxide. Experimental eye research. 2014; 129:74–82. [PubMed: 25446320]

[32]. Nieto, A.; Hou, H.; Sailor, MJ.; Freeman, WR.; Cheng, L. Engineered Porous Silicon Microparticle as Intravitreal Delivery System for Rapamycin. 2014.

[33]. Hou HY, Huffman K, Rios S, Freeman WR, Sailor MJ, Cheng L. A novel approach of daunorubicin application on formation of proliferative retinopathy using a porous silicon controlled delivery system: Pharmacodynamics. Investigative ophthalmology & visual science. 2015

[34]. Sailor, MJ. Porous Silicon in Practice: Preparation, Characterization, and Applications. Wiley-VCH; 2012.

[35]. Pacholski C, Sartor M, Sailor MJ, Cunin F, Miskelly GM. Biosensing using porous silicon double-layer interferometers: reflective interferometric Fourier transform spectroscopy. J Am Chem Soc. 2005; 127:11636–45. [PubMed: 16104739]

[36]. Chhablani J, Nieto A, Hou H, Wu EC, Freeman WR, Sailor MJ, et al. Oxidized Porous Silicon Particles Covalently Grafted with Daunorubicin as a Sustained Intraocular Drug Delivery System. Invest Ophthalmol Vis Sci. 2013; 54:1268–79. [PubMed: 23322571]

[37]. Hou H, Nieto A, Ma F, Freeman WR, Sailor MJ, Cheng L. Tunable sustained intravitreal drug delivery system for daunorubicin using oxidized porous silicon. J Control Release. 2014; 178:46–54. [PubMed: 24424270]

[38]. Wang CY, Hou H, Nan KH, Sailor MJ, Freeman WR, Cheng L. Intravitreal Controlled Release of Dexamethasone from Engineered Microparticles of Porous Silicon Dioxide. Investigative ophthalmology & visual science. 2014

[39]. Marney LC, Laha TJ, Baird GS, Rainey PM, Hoofnagle AN. Isopropanol protein precipitation for the analysis of plasma free metanephrines by liquid chromatography-tandem mass spectrometry. Clin Chem. 2008; 54:1729–32. [PubMed: 18687739]

[40]. Li YY, Kollengode VS, Sailor MJ. Porous silicon/polymer nanocomposite photonic crystals by microdroplet patterning. Adv Mater. 2005; 17:1249–51.

[41]. Herrero-Vanrell R, Bravo-Osuna I, Andres-Guerrero V, Vicario-de-la-Torre M, Molina-Martinez IT. The potential of using. biodegradable microspheres in retinal diseases and other intraocular pathologies. Prog Retin Eye Res. 2014; 42:27–43. [PubMed: 24819336]

[42]. Ma F, Nan K, Lee S, Beadle JR, Hou H, Freeman WR, et al. Micelle formulation of hexadecyloxypropyl-cidofovir (HDP-CDV) as an intravitreal long-lasting delivery system. European journal of pharmaceutics and biopharmaceutics : official journal of Arbeitsgemeinschaft fur Pharmazeutische Verfahrenstechnik eV. 2014

[43]. del Pozo-Rodriguez A, Delgado D, Gascon AR, Solinis MA. Lipid Nanoparticles as Drug/Gene Delivery Systems to the Retina. J Ocul Pharmacol Th. 2013; 29:173–88.

[44]. Nieto A, Hou H, Sailor MJ, Freeman WR, Cheng L. Ocular silicon distribution and clearance following intravitreal injection of porous silicon microparticles. Experimental eye research. 2013; 116:161–8. [PubMed: 24036388]

[45]. Noval AM, García R, Casas DR, Bayo DL, Vaquero VS, Costa VT, et al. Design and characterization of biofunctional magnetic porous silicon flakes. Acta Biomater. 2013; 9:6169–76. [PubMed: 23237987]

[46]. Berger MG, Dieker C, Thonissen M, Vescan L, Luth H, Munder H, et al. Porosity Superlattices - a New Class of Si Heterostructures. J Phys D-Appl Phys. 1994; 27:1333–6.

[47]. Parker AR, Mckenzie DR, Large MCJ. Multilayer reflectors in animals using green and gold beetles as contrasting examples. J Experimental Biol. 1998; 201:1307–13.

[48]. Rouf MA, Bilensoy E, Vural I, Hincal AA. Determination of stability of rapamycin following exposure to different conditions. European journal of pharmaceutical sciences. 2007; 32S:S22–S50.

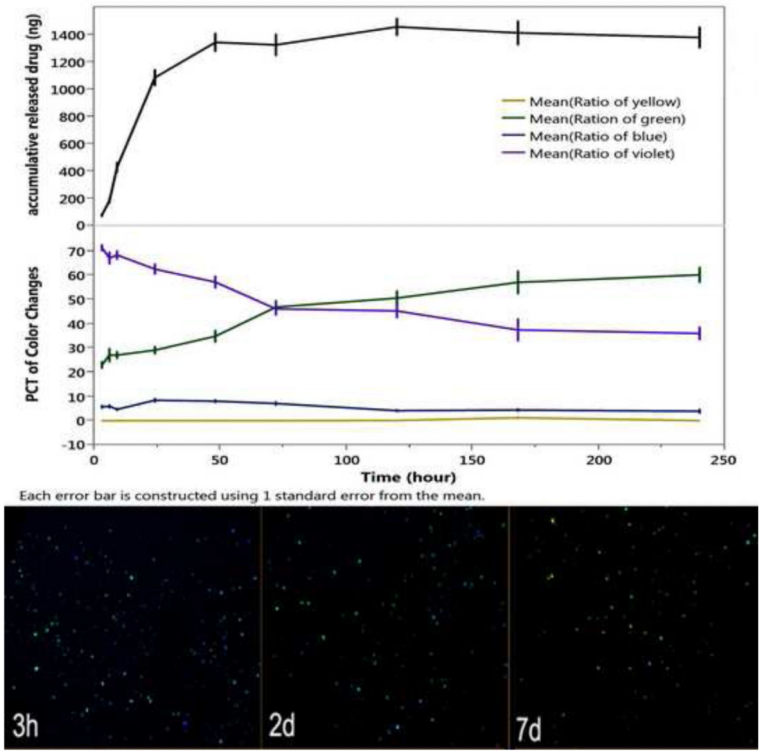

Figure 1.

Drug released and evolution of color classes as a function of time in HBSS at 37 °C for the 2.45-inf-RAP particle type. The green color component slowly increases while the violet component slowly decreases. Each color class is normalized such that the total color in all channels sums to 100% for each time point. The drug leaches out of the formulation more rapidly than the color changes. Each error bar is constructed using 1 standard error from the mean. Bottom images show the camera images obtained at the indicated time points. Samples are in a petri dish and imaged against a solid black background.

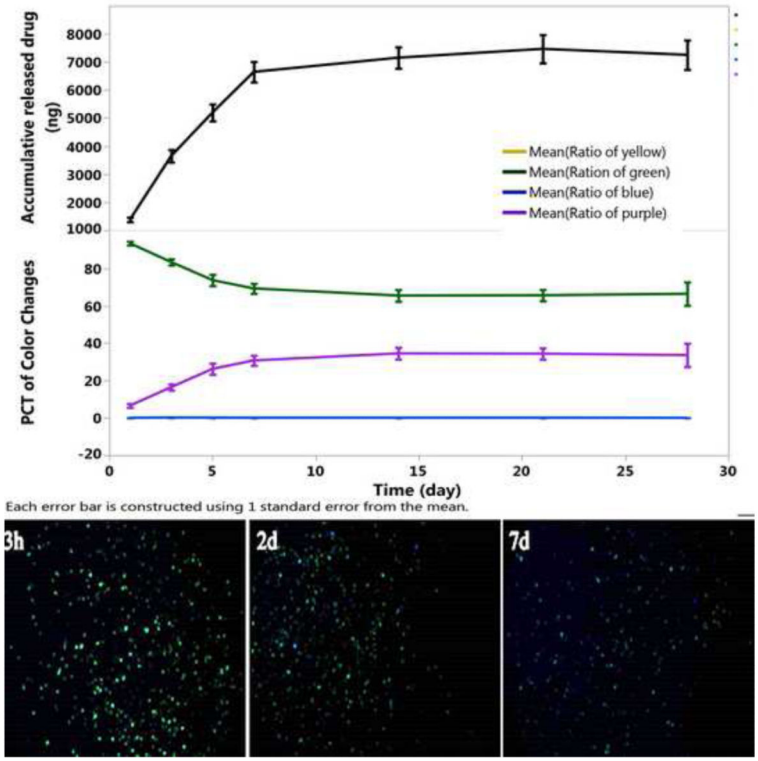

Figure 2.

Drug released and evolution of color classes as a function of time in HBSS at 37 °C for the 2.17-cov-DEX particle. The green color component slowly fades while the violet component slowly increases. Each color class is normalized such that the total color in all channels sums to 100% for each time point. Each error bar is constructed using 1 standard error from the mean. Bottom images show the camera images obtained at the indicated time points. Samples are in a petri dish and imaged against a solid black background.

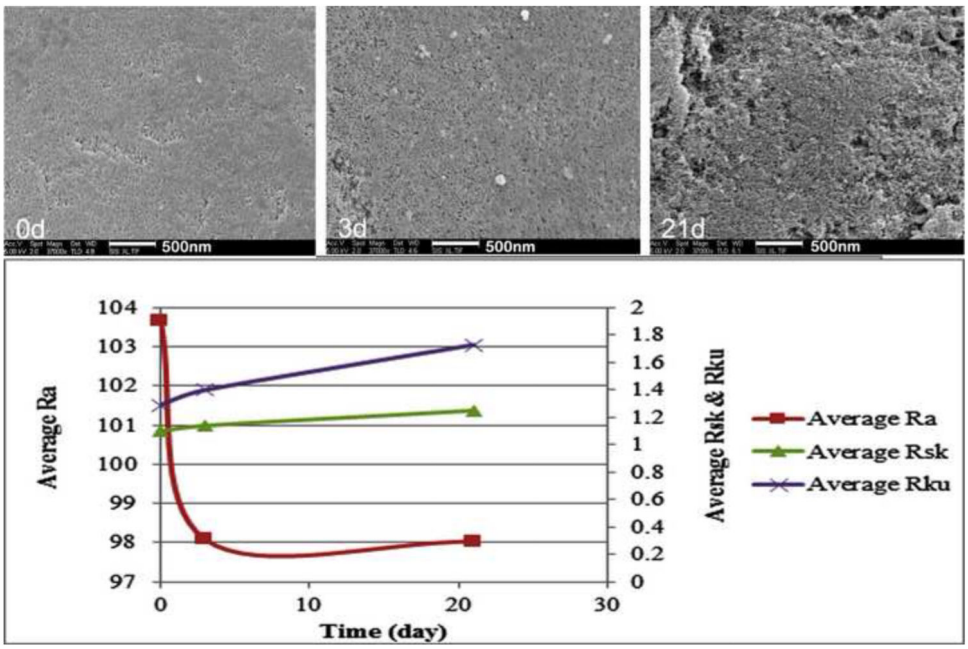

Figure 3.

SEM images and roughness analysis of the 2.45-inf-RAP particles measured *ex-situ* during the course of an *in vitro* drug release experiment (HBSS, 37 °C). Ra: Arithmetical mean deviation of the roughness profile; Rsk: Skewness of the roughness profile; Rku: Kurtosis of the roughness profile. The 21-day image demonstrated obvious pSi erosion compared with 0-day samples. Due to the unevenness erosion, Ra did not well capture the profile change; but both Rsk and Rku showed elevation, indicating presence of high spikes and deep valleys on the 21-day sample.

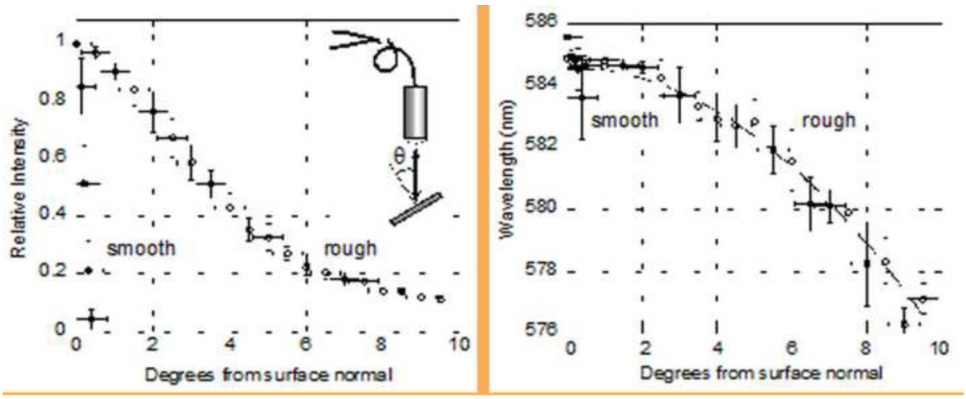

Figure 4.

Intensity and wavelength of the stop band reflected from smooth (solid circles) and roughened (open circles) porous Si rugate filter samples, as a function of angle relative to the surface normal. A specular reflection corresponds to 0 degrees from the surface normal. For this sample, roughening is achieved by spray-coating with a fine mist of micron-scale polymer droplets [40]. Inset shows the optical setup used, including the sample, lens, and bifurcated fiber optic cable. In this experiment the observation axis is coaxial with the illumination axis, the diameter of the light spot on the sample is 0.74 cm, and the sample-lens distance is 56.7 cm.

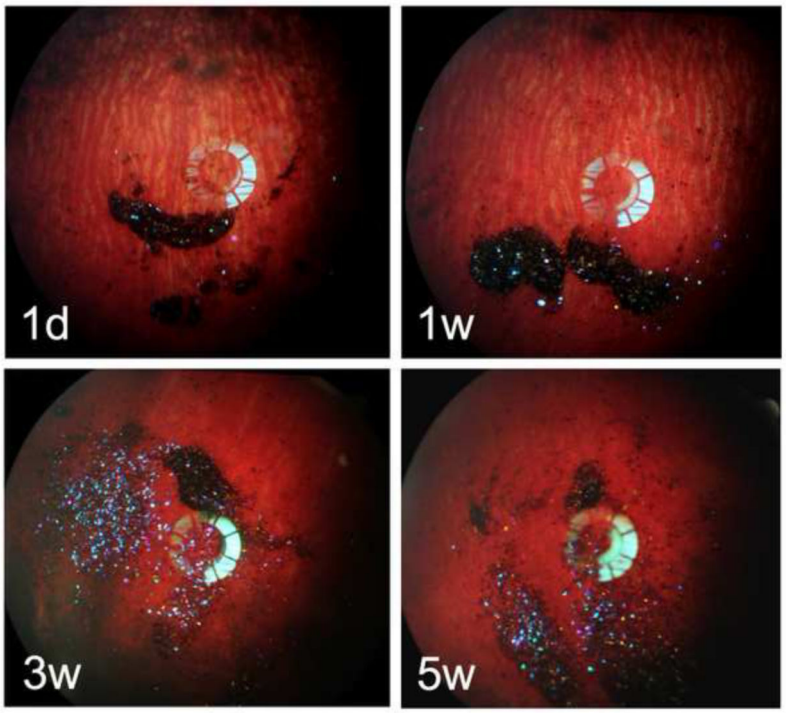

Figure 5.

Fundus photographs of the rabbits, monitored for 5 weeks post-injection of the 2.45-inf-RAP particle formulation. The particles show up as dark or predominantly violet colored features in the images. Each image is from a different rabbit, which was sacrificed immediately after the image acquisition to obtain drug concentration (Figure 5) at the indicated time point.

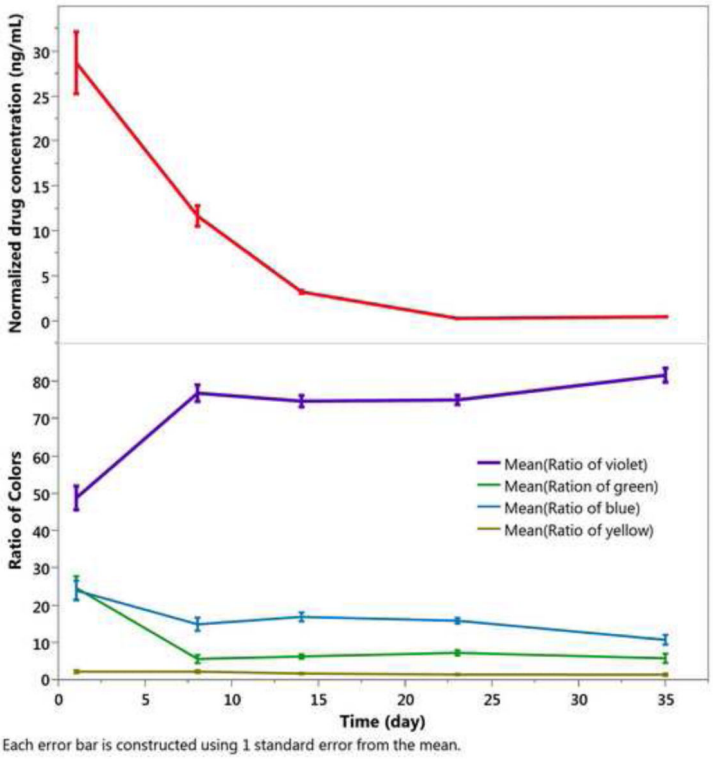

Figure 6.

Drug released and evolution of color classes as a function of time *in vivo* for the 2.45-inf-RAP pSi particle type injected into rabbit eyes at day 0. Each color class is normalized such that the total color in all channels sums to 100% for each time point. Each error bar is constructed using 1 standard error from the mean.

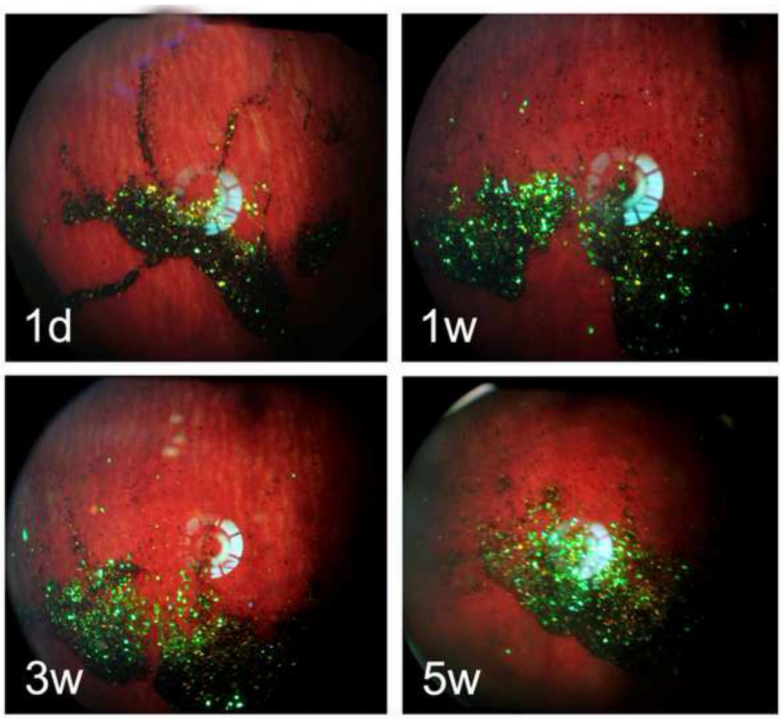

Figure 7.

Fundus photographs of rabbits monitored for 5 weeks post-injection of the 2.17-inf-RAP particle formulation. The particles show up as dark or predominantly violet colored features in the images. Each image is from a different rabbit, which was sacrificed immediately after the image acquisition to obtain drug concentration at the indicated time point.

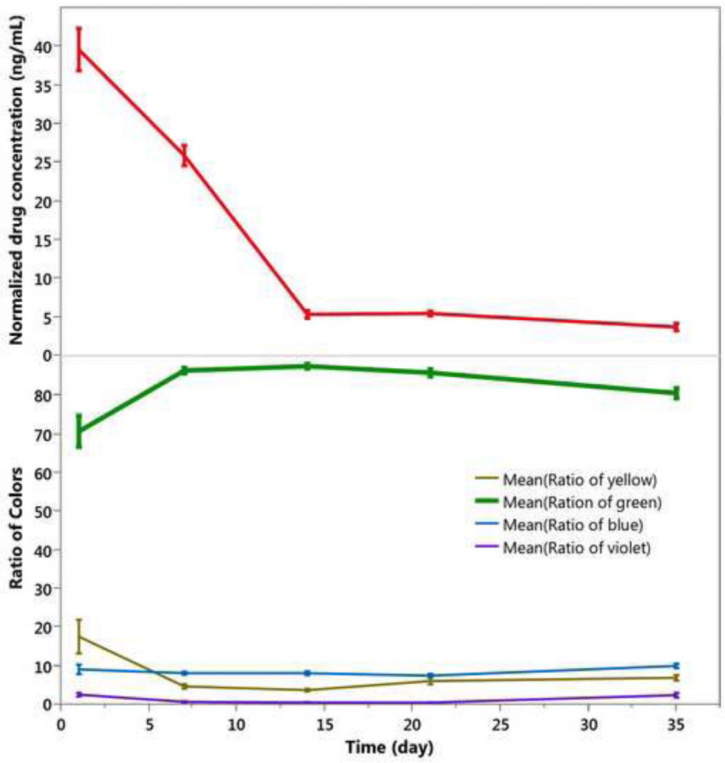

Figure 8.

Drug released and evolution of color classes as a function of time *in vivo* for the 2.17-inf-RAP pSi particle type injected into rabbit eyes at day 0. Each color class is normalized such that the total color in all channels sums to 100% for each time point. Each data point represents three rabbits, which were sacrificed at the indicated time points to obtain drug concentration. Each error bar is constructed using 1 standard error from the mean.

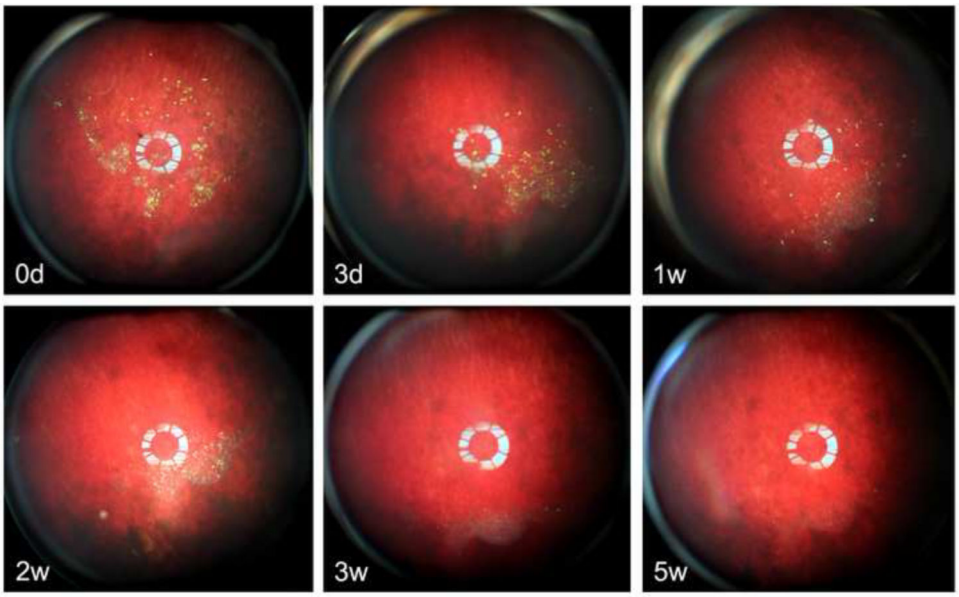

Figure 9.

Fundus photographs of six separate rabbits, monitored for 5 weeks post-injection of the 2.17-cov-DEX particle formulation. The particles show up as yellow-green colored features in the images. Each image is from a different rabbit, which was sacrificed immediately after the image acquisition to obtain drug concentration at the indicated time point.

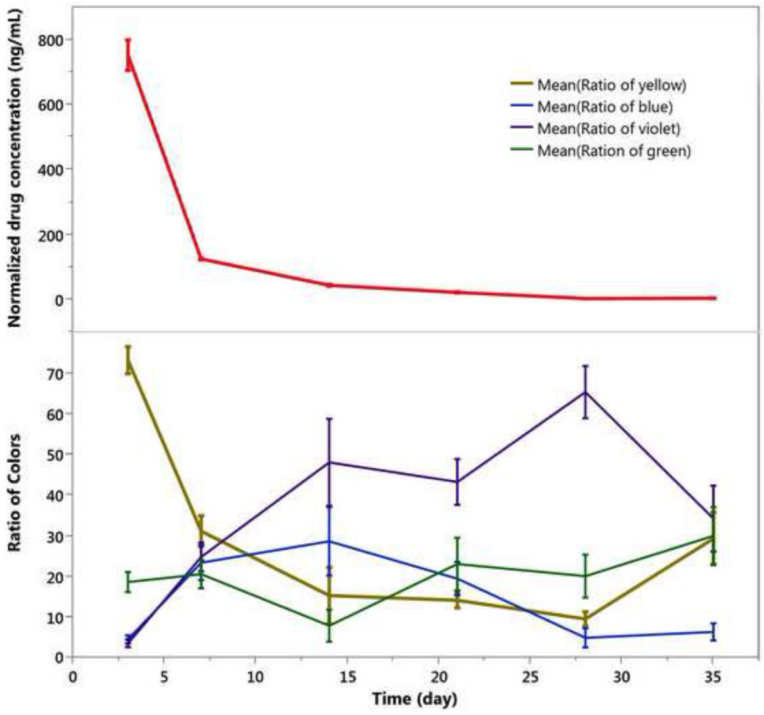

Figure 10.

Drug released and evolution of color classes as a function of time *in vivo* for the 2.17-cov-DEX particle type injected into rabbit eyes at day 0. Each color class is normalized such that the total color in all channels sums to 100% for each time point. Each data point represents three rabbits, which were sacrificed at the indicated time points to obtain drug concentration. Particle colors was shifted from yellow to violet during the 5-week observation period. Each error bar is constructed using 1 standard error from the mean.

Table 1

pSi particle size information

***k* value**	**Thickness (μm)**	**length (μm)**	**width (μm)**
2.17	21.9±1.4	52.6±13.7	36.5±10.4
2.45	27.9±1.4	70.9±17.7	43.8±8.0

pSi: porous silicon

Table 2

Peak reflectance of pSi and $pSiO_2$ films in different media

K value	Average reflectance peak in air			Average reflectance peak in deionized water			Average reflectance peak in PBS			Shift from air to PBS	
	fresh	oxidized	shift	fresh	oxidized	shift	fresh	oxidized	shift	fresh	oxidized
2.17	615±9.29 (orange)	510±6.58[#] 501±3.7[*]	−105[#] −114[*]	672±20.60 (red)	565±6.71[#] 551±3.51[*] (green)	−107[#] −122[*]	687±7.79 (red)	561±2.45[#] 551±7.67[*] (green)	−126[#] −136[*]	−72	−51 −50[*]
2.25	609±4.01 (orange)	494±2.56 (cyan)	−115	669±2.88 (red)	553±3.33 (green)	−94	673±2.15 (red)	553±3.10 (green)	−120	−64	−59
2.35	597±3.71 (orange)	482±3.77 (blue)	−115	654±5.74 (red)	538±5.38 (green)	−117	651±5.03 (red)	533±4.45 (green)	−112	−54	−51
2.45	556±5.33 (green)	438±6.2 (violet)	−117	609±9.26 (orange)	491±8.33 (cyan)	−118	612±6.18 (orange)	491±8.58 (cyan)	−121	−56	−53
2.55	530±1.13 (green)	425±2.73 (violet)	−105	577±5.27 (yellow)	472±3.21 (blue)	−105	581±2.45 (yellow)	476±3.15 (blue)	−105	−51	−51

[#]Film oxidized at 600 °C for 1 hour

[*]Film oxidized at 800 °C for 2 hours

−:blue shift

+: red shift

Table 3

Particle parameters and drug loading efficiency

Particle	Si wafer resistivity (mΩ·cm)	*k* value	Thickness (μm)	Porosity (%)	Model drug	Loading method	Loading efficiency (μg/mg)
2.45-inf-RAP	1.23	2.45	27.92±1.37	44.5±1.90	Rapamycin	infiltration	73±9
2.17-inf-RAP	1.29	2.17	21.94±1.43	50.4±1.67	Rapamycin	infiltration	86±7
2.17-cov-DEX	1.29	2.17	21.94±1.43	50.4±1.67	Dexamethasone	covalent	80±19